4.7. The 2017 coastal El Niño

Authors: Florent Gasparin, Vincent Echevin, Alexandre Mignot, Coralie Perruche, Marie Drévillon

Statement of main outcome: While the Tropical Pacific was rather in neutral El Niño-Southern Oscillation conditions during 2017, a significant surface warming with similar amplitude to typical eastern Pacific El Niños was found locally along the coast of Peru and Ecuador at the beginning of the year. Triggered by an anomalously low along-shore wind, the surface warming stopped the coastal upwelling and generated strong interannual precipitation over the coastal land in the north of Peru. This warm event, named 'coastal El Niño', was not anticipated by climate forecasting centres and left local authorities totally unprepared, regarding floods and landslides generated by persistent heavy rains from January to March.Given the strong consequences for the local populations, these very rare coastal El Niños (only two previously reported) therefore require further investigations.

Products used:

Ref. no.	Product name and type	Documentation
4.7.1.	GLOBAL_REANALYSIS_PHY_001_025	PUM: http://marine.copernicus.eu/documents/PUM/CMEMS-GLO-PUM-001-025.pdf QUID: http://marine.copernicus.eu/documents/QUID/CMEMS-GLO-QUID-001-025.pdf
4.7.2.	ECMWF Era-Interim reanalysis wind product Reanalysis (atmosphere)	Dee et al. (2011), downloaded from the website http://data.ecmwf.int/data/
4.7.3	OCEANCOLOUR_GLO_CHL_L4_REP_OBSERVATIONS_009_082 OCEANCOLOUR_GLO_CHL_L4_NRT_OBSERVATIONS_009_033	PUM: http://marine.copernicus.eu/documents/PUM/CMEMS-OC-PUM-009-ALL.pdf QUID: http://marine.copernicus.eu/documents/QUID/CMEMS-OC-QUID-009-033-037-082-098.pdf http://marine.copernicus.eu/documents/QUID/CMEMS-OC-QUID-009-030-032-033-081-082-083-085-086.pdf
4.7.4	GLOBAL_REANALYSIS_BIO_001_018	PUM: http://marine.copernicus.eu/documents/PUM/CMEMS-GLO-PUM-001-018.pdf QUID : http://marine.copernicus.eu/documents/QUID/CMEMS-GLO-QUID-001-018.pdf

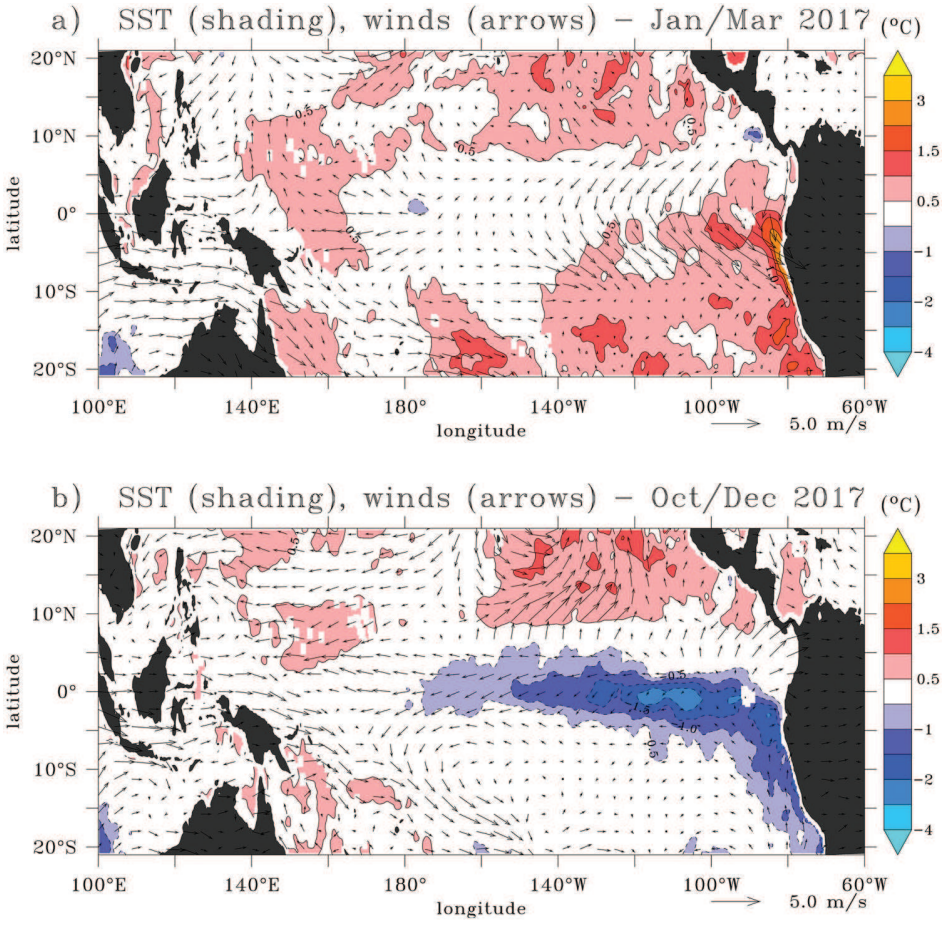

Figure 4.7.1. Temperature (shading, in °C) and winds (arrows, in m/s) anomalies, from the 1993–2014 climatology, time-averaged for the periods (b) January–March 2016 and (c) October–December 2016 (products reference 4.7.1, 4.7.2).

As the dominant interannual climate signal on Earth, the El Niño-Southern Oscillation includes a wide variety of local and large-scale atmospheric and oceanic phenomena, but is typically characterised by two anomalous basin-wide patterns in the tropical Pacific (e.g., Guilyardi et al. 2009; Wang et al. 2017 for a review). At the beginning of 2017, while the tropical Pacific conditions in 2017 were not marked by significant anomalous basin-wide El Niño-Southern Oscillation conditions such as during the 2015/2016 El Niño (Gasparin et al. 2017), a localised warm event, associated with anomalously strong precipitation, occurs in the southeastern Pacific along the northwestern coast of South America. This type of event, named 'coastal El Niño', is very rare and the mechanisms are not well known, as only two coastal El Niños were previously reported in 1891 and 1925 (Takahashi and Martínez 2017).

As seen in Figure 4.7.1, the January/March 2017 sea surface temperature is characterised by a strong warm anomaly of more than 4°C in the eastern equatorial Pacific off the coasts of Peru and Ecuador. This anomaly was similar in shape and intensity to anomalies typical of eastern Pacific El Niño conditions, with the major difference being the absence of El Niño conditions in the central-eastern Pacific during this period. Although a relatively weak downwelling equatorial Kelvin wave may have contributed to the warm sea surface temperature anomaly along the Peru coasts in February–March 2017 (through the deepening of the thermocline), the main forcing triggering the 2017 event was potentially a strong large-scale relaxation of the southeasterly trades in the eastern south Pacific (Figure 4.7.1). The large-scale mechanism which generated the wind decrease could be an enhanced deep convection over north Australia, triggering an atmospheric teleconnection between the western equatorial Pacific and the eastern South Pacific, as evidenced by Garreaud (2018).

The intense local ocean warming, which peaked during March 2017, resulted in enhanced local precipitation rate in the northern Peru and Ecuador. In Figure 4.7.2, the precipitation rate time series, area-averaged off the coasts of Peru (red box in Figure 4.7.2 (a)), shows that the March 2017 precipitation rate was more than 4 times higher than normal, exhibiting larger amplitude as for the 1997/1998 El Niño. This impacted on the surface ocean in favouring the development of a negative sea surface salinity anomaly along the coast of Peru (Figure 4.7.2(a)). In addition to the coastal area, this strong event caused high inland precipitation over the nearby desert land inducing devastating floods and 'huacos' (rivers of mud) in northern Peru and Ecuador (Fraser 2017). Further investigations would require to quantify the dominant terms of the freshwater balance in the surface layer, including both atmospheric inputs and oceanic dynamics.

To further investigate how this event impacted on the phytoplankton biomass and the production of organic carbon through photosynthesis, the surface chlorophyll concentration (used as a proxy of phytoplankton biomass) is shown from independent estimates deduced from satellite observations and from a numerical model (Figure 4.7.3). A strong negative anomaly (<2.2 mg/m^3) clearly appears along the coast of Peru on both estimates. The model estimate suggests that this negative anomaly is extended down to about 30 m depth. The coastal upwelling system off Peru is a place of enhanced level of primary production due to high nutrient supply by wind-driven upwelling (Pennington et al. 2006). In March 2017, a decrease of the nearshore wind-driven upwelling along the coast of Peru (Figure 4.7.3(c)), associated with Ekman pumping changes (Echevin et al. 2018), probably reduced the inputs of nutrients to the surface layer, therefore decreasing the production of organic carbon and phytoplankton biomass.

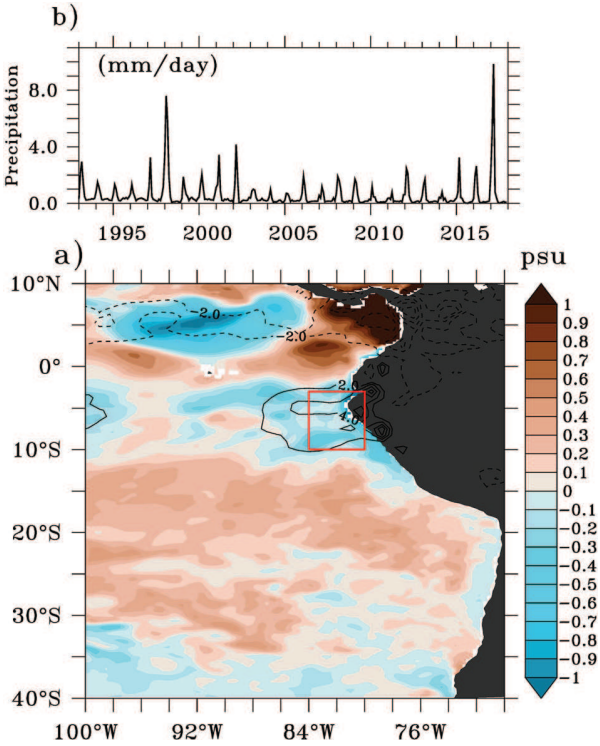

Figure 4.7.2. (a) Salinity anomaly (shading) and precipitation rate (contour, in mm/day), for the month of March 2017 (products reference 4.7.1, 4.7.2). (b) Precipitation rate is area-averaged in the red box of (a) (84°W–80°W, 3°S–10°S). Anomaly is calculated from the 1993–2014 climatology.

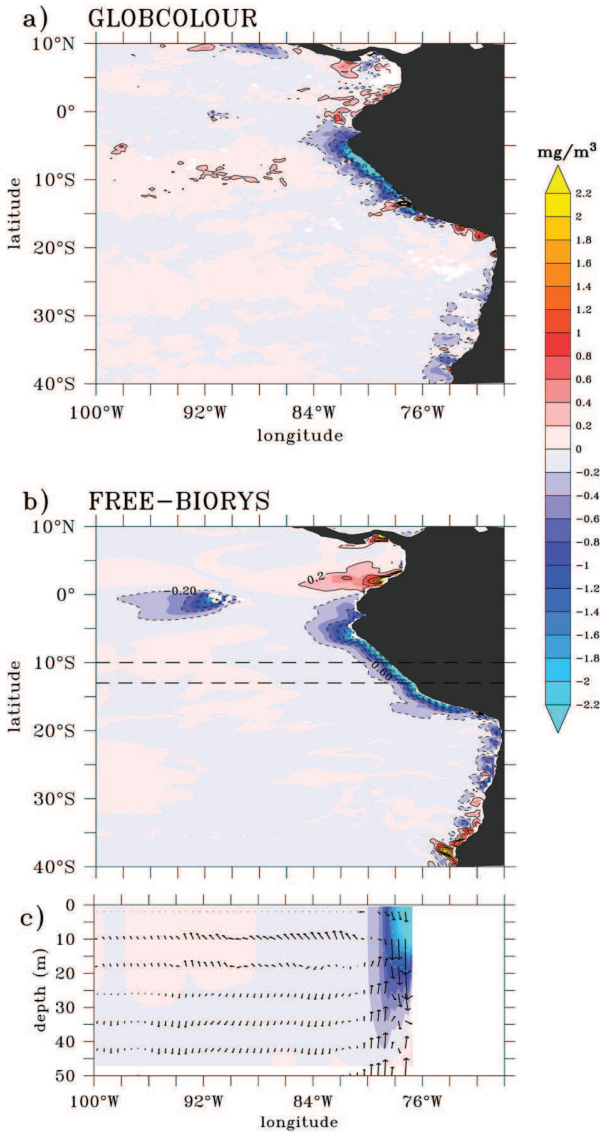

Figure 4.7.3. (a, b) Surface chlorophyll concentration anomalies (in mg/m^3), from the 2007–2017 climatology, for the month of March 2017 from (a) GLOBCOLOUR, and (b) the FREE-BIORYS product (products reference 4.7.3, 4.7.4). (c) Vertical section of chlorophyll concentration anomaly (shading) and current velocity anomaly (arrows), latitude-averaged over 10°S–13°S (dashed lines in b) in the upper 50 m. Anomalies are calculated from the climatological cycle. The current velocity has been vertically interpolated every 8 m.

Thus, the large-scale atmospheric variability in the eastern Pacific has led to significant modification of the local oceanic/land conditions (i) by warming coastal surface waters and (ii) by enhancing precipitation in the northern Peru and Ecuador, and (iii) by decreasing the upwelling-driven primary production in the coastal ocean. Unlike the very strong 2015/2016 El Niño, the 2017 coastal El Niño was not anticipated by climate forecasting centres and left local authorities totally unprepared (Ramírez and Briones 2017; Garreaud 2018). Although the combination of oceanic/atmospheric observation and model products allows a detailed description of the 2017 coastal El Niño event, the rare occurrence of these coastal El Niños can make difficult the understanding and the prediction of these extreme events, which thus require further investigation.

References

Section 4.1. Weddell Sea Polynya

Blanke B, Delecluse P. 1993. Variability of the tropical Atlantic-Ocean simulated by a general-circulation model with 2 different mixed-layer physics. J Phys Oceanogr. 23:1363–1388.

Carsey FD. 1980. Microwave observation of the Weddell polynya. Month Weath Rev. 108:2032–2044.

Cavalieri DJ, Martin S. 1994. The contribution of Alaskan, Siberian, and Canadian coastal polynyas to the cold halocline layer of the Arctic Ocean. J Geophys Res Oceans. 99:18343–18362.

Cheon WG, Park YG, Toggweiler JR, Lee SK. 2014. The relationship of Weddell polynya and open-ocean deep convection to the southern hemisphere westerlies. J Phys Oceanogr. 44:694–713.

Comiso JC, Gordon AL. 1987. Recurring polynyas over the Cosmonaut Sea and the Maud Rise. J Geophys Res Oceans. 92:2819–2833.

Dufour CO, Morrison AK, Griffies SM, Frenger I, Zanowski H, Winton M. 2017. Preconditioning of the Weddell Sea polynya by the ocean mesoscale and dense water overflows. J Clim. 30:7719–7737.

Gordon AL, Visbeck M, Comiso JC. 2007. A possible link between the Weddell polynya and the southern annular mode. J Clim. 20:2558–2571.

Heuzé C, Heywood KJ, Stevens DP, Ridley JK. 2013. Southern ocean bottom water characteristics in CMIP5 models. Geophys Res Lett. 40:1409–1414.

Heuzé C, Ridley JK, Calvert D, Stevens DP, Heywood KJ. 2015. Increasing vertical mixing to reduce southern ocean deep convection in NEMO3.4. Geosci Model Dev. 8:3119.

Holland DM. 2001. Explaining the Weddell polynya – a large ocean eddy shed at Maud Rise. Science. 292:1697–1700.

Kjellsson J, Holland PR, Marshall GJ, Mathiot P, Aksenov Y, Coward AC, Bacon S, Megann AP, Ridley JK. 2015. Model sensitivity of the Weddell and Ross seas, Antarctica, to vertical mixing and freshwater forcing. Ocean Model. 94:141–152.

Kusahara K, Hasumi H, Tamura T. 2010. Modeling sea ice production and dense shelf water formation in coastal polynyas around East Antarctica. J Geophys Res Oceans. 115: C10006.

Lindsay RW, Holland DM, Woodgate RA. 2004. Halo of low ice concentration observed over the Maud Rise seamount. Geophys Res Lett. 31:L13302.

Martin T, Park W, Latif M. 2013. Multi-centennial variability controlled by Southern Ocean convection in the Kiel climate model. Clim Dynam. 40:2005–2022.

Martinson DG, Killworth PD, Gordon AL. 1981. A convective model for the Weddell polynya. J Phys Oceanogr. 11:466–488.
Morales-Maqueda MA, Willmott AJ, Biggs NRT. 2004. Polynya dynamics: a review of observations and modeling. Rev Geophys. 42:RG1004.
Orsi AH, Jacobs SS, Gordon AL, Visbeck M. 2001. Cooling and ventilating the abyssal ocean. Geophys Res Lett. 28:2923–2926.
Smith WO Jr, Barber D. 2007. Polynyas: windows to the world. Amsterdam: Elsevier.
Swart S, Campbell EC, Heuzé C, Johnson K, Lieser JL, Massom M, Mazloff M, Meredith M, Reid P, Sallée J-B, Stammerjohn S. 2018. Return of the Maud Rise polynya: climate litmus or sea ice anomaly? State of the Climate in 2017. BAMS. 48.

Section 4.2. T/S anomalies in the North Atlantic subpolar gyre

Barrier N, Cassou C, Deshayes J, Treguier AM. 2014. Response of North Atlantic Ocean circulation to atmospheric weather regimes. J Phys Oceanogr. 44:179–201. doi:10.1175/JPO-D-12-0217.1.
Belkin IM, Levitus S, Antonov J, Malmberg SA. 1998. 'Great salinity anomalies' in the North Atlantic. Prog Oceanogr. 41(1):1–68.
Czaja A, Frankignoul C. 2002. Observed impact of Atlantic SST anomalies on the North Atlantic oscillation. J Clim. 15:606–623.
Deshayes J, Frankignoul C. 2008. Simulated variability of the circulation in the North Atlantic from 1953 to 2003. J Clim. 21:4919–4933. doi:10.1175/2008JCLI1882.1.
Dickson RR, Meincke J, Malmberg SA, Lee AJ. 1988. The 'great salinity anomaly' in the northern North Atlantic 1968–1982. Prog Oceanogr. 20(2):103–151.
Flatau MK, Talley L, Niiler PP. 2003. The North Atlantic oscillation, surface current velocities, and SST changes in the subpolar North Atlantic. J Clim. 16(14):2355–2369.
Gourrion J, Deshayes J, Juza M, Szekely T, Tintoré J. 2018. A persisting regional cold and fresh water anomaly in the Northern Atlantic. In: Copernicus marine service ocean state report, issue 2. J Oper Oceanogr. 11(sup1):s125–s129. doi:10.180/1755876X.2018.1489208.
Grist JP, Josey SA, Jacobs ZL, Marsh R, Sinha B, Van Sebille E. 2016. Extreme air–sea interaction over the North Atlantic subpolar gyre during the winter of 2013–2014 and its sub-surface legacy. Clim dyn. 46(11–12):4027–4045.
Hátún H, Sandø AB, Drange H, Hansen B, Valdimarsson H. 2005. Influence of the Atlantic subpolar gyre on the thermohaline circulation. Science. 309(5742):1841–1844.
Josey SA, Hirschi JJM, Sinha B, Duchez A, Grist JP, Marsh R. 2018. The recent Atlantic cold anomaly: causes, consequences, and related phenomena. Ann Rev Mar Sci. 10:475–501.
Levitus S, Antonov JI, Boyer TP, Locarnini RA, Garcia HE, Mishonov AV. 2009. Global ocean heat content 1955–2008 in light of recently revealed instrumentation problems. Geophys Res Lett. 36:L07608. doi:10.1029/2008GL037155.
Piecuch CG, Ponte RM, Little CM, Buckley MW, Fukumori I. 2017. Mechanisms underlying recent decadal changes in subpolar North Atlantic Ocean heat content. J Geophys Res Oceans. 122(9):7181–7197.
Robson J, Ortega P, Sutton R. 2016. A reversal of climatic trends in the North Atlantic since 2005. Nat Geosci. 9(7):513.
Robson J, Sutton R, Lohmann K, Smith D, Palmer MD. 2012. Causes of the rapid warming of the North Atlantic Ocean in the mid-1990s. J Clim. 25(12):4116–4134.
Zunino P, Lherminier P, Mercier H, Daniault N, García-Ibáñez MI, Pérez FF. 2017. The GEOVIDE cruise in May–June 2014 reveals an intense meridional overturning circulation over a cold and fresh subpolar North Atlantic. Biogeosciences. 14:5323–5342. doi:10.5194/bg-14-5323-2017.

Section 4.3. Anticyclonic Eddy Anomaly: impact on the boundary current and circulation in the western Mediterranean Sea

Amores A, Monserrat S, Marcos M. 2013. Vertical structure and temporal evolution of an anticyclonic eddy in the Balearic Sea (western Mediterranean). J Geophys Res Oceans. 118:2097–2106.
Bouffard J, Pascual A, Ruiz S, Faugère Y, Tintoré J. 2010. Coastal and mesoscale dynamics characterization using altimetry and gliders: A case study in the Balearic Sea. J Geophys Res Oceans. 115:C10029.
Dengler M, Schott FA, Eden C, Brandt P, Fischer J, Zantopp RJ. 2004. Break-up of the Atlantic deep western boundary current into eddies at 8° S. Nature. 432:1018–1020.
Escudier R, Renault L, Pascual A, Brasseur P, Chelton D, Beuvier J. 2016. Eddy properties in the western Mediterranean Sea from satellite altimetry and a numerical simulation. J Geophys Res Oceans. 121:3990–4006.
Font J, Salat J, Tintoré J. 1988. Permanent features of the circulation in the Catalan Sea. Oceanol Acta Spec issue.
Garreau P, Garnier V, Schaeffer A. 2011. Eddy resolving modelling of the Gulf of Lions and Catalan Sea. Ocean Dyn. 61(7):991–1003.
Greatbatch RJ. 1987. A model for the inertial recirculation of a gyre. J Mar Res. 45:601–634.
Herbaut C, Martel F, Crépon M. 1997. A sensitivity study of the general circulation of the western Mediterranean Sea. Part II: the response to atmospheric forcing. J Phys Oceanogr. 27:2126–2145.
Heslop EE, Ruiz S, Allen J, López-Jurado JL, Renault L, Tintoré J. 2012. Autonomous underwater gliders monitoring variability at 'choke points' in our ocean system: a case study in the western Mediterranean Sea. Geophys Res Lett. 39:L20604.
Hogg NG, Stommel H. 1985. On the relation between the deep circulation and the Gulf Stream. Deep Sea Res Part Oceanogr Res Pap. 32:1181–1193.
Holland WR. 1978. The role of mesoscale eddies in the general circulation of the ocean—numerical experiments using a wind-driven quasi-geostrophic model. J Phys Oceanogr. 8:363–392.
Holland WR, Lin LB. 1975. On the generation of mesoscale eddies and their contribution to the oceanic general circulation. II A parameter study. J Phys Oceanogr. 5:658–669.

VOL. 12, NO. S1, SEPTEMBER 2019

COPERNICUS MARINE SERVICE OCEAN STATE REPORT, ISSUE 3

Editors

Karina von Schuckmann Pierre-Yves Le Traon

Review Editors

Neville Smith (Chair) Ananda Pascual Samuel Djavidnia

Jean-Pierre Gattuso Marilaure Grégoire Glenn Nolan

To cite the entire report

How to cite the entire report: von Schuckmann, K., P.-Y. Le Traon, N. Smith, A. Pascual, S. Djavidnia, J.-P. Gattuso, M. Grégoire, G. Nolan (2019) Copernicus Marine Service Ocean State Report, Issue 3, Journal of Operational Oceanography, 12:sup1, s1–s123; DOI: 10.1080/1755876X.2019.1633075

To cite a specific section in the report (example)

Raudsepp, U., I. Maljutenko, M. Kõuts (2019). Cod reproductive volume potential in the Baltic Sea. In: Copernicus Marine Service Ocean State Report, Issue 3, Journal of Operational Oceanography, 12:sup1, s26–s30; DOI: 10.1080/1755876X.2019.1633075